

Electronic supplementary information

**Switchable synthesis of furfurylamine and
tetrahydrofurfurylamine from furfuryl alcohol over
Raney Nickel**

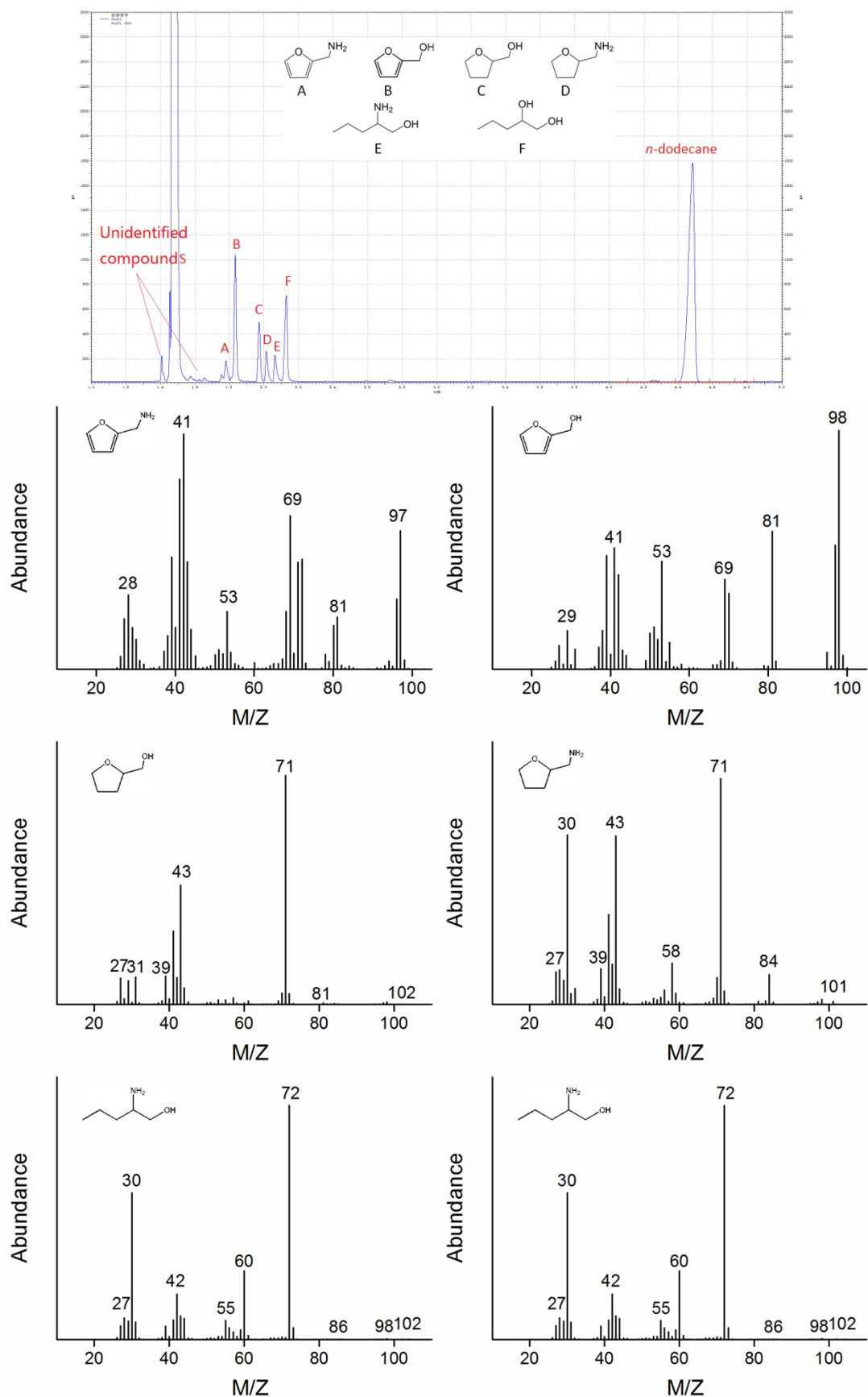


Fig.S1 GC spectrum and mass spectra of the main reaction components for FA amination.

Table S1(a) Reported adsorption energy of NH₃ on different metal surface

Computational Model	Adsorption site	Adsorption energy (eV)						Reference
		Rh	Ru	Pt	Pd	Co	Ni	
2×2 unit cell, 4 layers slabs	(100) top	0.85		0.79	0.66			1
2×2 unit cell, 4 layers slabs	(111) top	0.79		0.70	0.57			1
2×2 unit cell, 3 layer slabs	(111) top	0.87						2
2×2 unit cell, 5 layers slabs	(111) top	0.75						3
2×2 unit cell, 6 layers slabs	(111) top	0.73						4
2×2 unit cell, 6 layers slabs	(100) top	0.84						4
2×2 unit cell, 2 layers slabs	(0001) top		1.32					5
3×2 unit cell, 3 layers slabs	(0001) top		0.89					6
Ru ₁₃ (7,6) cluster	(001) top		1.14					7
2×2 unit cell, 4 layers slabs	(111) top			0.75				8
2×2 unit cell, 4 layers slabs	(100) top			0.89				8
2×2 unit cell, 5 layers slabs	(111) top			0.70				9
2×2 unit cell, 4 layers slabs	(100) top			0.79				10
2×2 unit cell, 3 layers slabs	(111) top			0.78				11
2×2 unit cell, 5 layers slabs	(111) top				0.68	0.83		12
3×2 unit cell, 4 layers slabs	(111) top				0.84			13
2×2 unit cell, 4 layers slabs	(111) top				0.62			14
3×3 unit cell, 4 layers slabs	(111) top					0.68	0.75	15
4×2 unit cell, 4 layers slabs	(0001) top					0.61		16
2×2 unit cell, 5 layers slabs	(111) top						0.68	17

3×2 unit cell, 4 layers slabs	(111) top		0.88	17
Ni ₂₈ cluster	(111) top		0.84	17
3×3 unit cell, 5 layers slabs	(110) top		0.90	18
2×2 unit cell, 5 layers slabs	(111) top		0.88	19
3×3 unit cell, 5 layers slabs	(111) top		0.91	20

Table S1(b) Reported adsorption energy of H₂ on different metal surface

Computational Model	Adsorption site	Adsorption energy (eV)						Reference
		Rh	Ru	Pt	Pd	Co	Ni	
2×2 unit cell, 3 layers slabs	(111) hole	0.33	0.41	0.37	0.42	0.31	0.37	21
3×3 unit cell, 7 layers slabs	(100)hollow	0.42			0.47			22
1×1 unit cell, 6 layers slabs	(001)FCC hollow		0.573					23
1×2 unit cell, 6 layers slabs	(001) FCC hollow		0.603					23
($\sqrt{3} \times \sqrt{3}$)R30°, 6 layers slabs	(001) FCC hollow		0.593					23
2×2 unit cell, 3 layers slabs	(111) top			0.46				24
2×2 unit cell, 5 layers slabs	(111)hollow			0.44				25
2×2 unit cell, 3 layers slabs	(111) top			0.52				26
(111)hollow $\sqrt{3} \times \sqrt{3}$ unit cell, 3 layers slabs	(111)hollow			0.52				27
2×2 unit cell, 3 layers slabs	(111)hollow			0.55				27
3×2 $\sqrt{3}$ unit cell, 3 layers slabs	(111)hollow			0.59				27
1×1 unit cell, 5 layers slabs	(111)FCC hollow				0.51			28
1×1 unit cell, 8 layers slabs	(100) FCC hollow				0.52			28

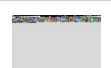
1×1 unit cell, 5 layers slabs	(110) pseudo 3-fold	0.50		28
2×2 unit cell, 3 layers slabs	(111) FCC hollow	0.51	0.66	24
2×2 unit cell, 5 layers slabs	(111) FCC hollow	0.50	0.65	25
2×2 unit cell, 5 layers slabs	(111) FCC hollow	0.54		29
2×2 unit cell, 5 layers slabs	(100) FCC hollow	0.52		29
2×2 unit cell, 5 layers slabs	(100) FCC hollow	0.49		30
2×2 unit cell, 5 layers slabs	(111) FCC hollow	0.48		31
2×2 unit cell, 4 layers slabs	(100) FCC hollow	0.46		31
2×1 unit cell, 6 layers slabs	(0001) FCC hollow	0.46		32
1×1 unit cell, 6 layers slabs	(0001) FCC hollow	0.48		32
8×8 unit cell, 4 layers slabs	(111) FCC hollow	0.572		33
12×12 unit cell, 4 layers slabs	(111) FCC hollow	0.567		33
16×16 unit cell, 4 layers slabs	(111) FCC hollow	0.568		33
12×12 unit cell, 6 layers slabs	(111) FCC hollow	0.573		33
2×2 unit cell, 4 layers slabs	(111) FCC hollow	0.62		34

Table S2 Reductive amination of furfural into furfural under different reaction conditions

Entry	H ₂ (MPa)	Conv. (%)	Select. (%)		
					Imines
1	0.1	100	62.6	-	37.4
2	0.5	100	100	-	-
3	1.0	100	100	-	-
4	2.0	100	80.7	19.3	-

Reaction conditions: Furfural, 0.5 g; THF, 15 mL; Raney Ni, 0.25 g; NH₃ pressure, 0.35 MPa; temperature, 80 °C; reaction time, 2 h; stirring speed, 1200 rpm.

Table S3 Confirmation of the “borrowing H₂” mechanism

Entry	Reagent	Conv. (%)	Yield. (%)		
					
1	NH ₃	24.0	-	22.2	1.8
2 ^a	cyclohexene	7.6	7.6	-	-
3 ^b	-	0	-	-	-

Reaction conditions: Furfuryl alcohol, 0.5 g; THF, 15 mL; Raney Ni, 0.25 g; temperature, 160 °C; reaction time, 24 h; stirring speed, 1200 rpm. ^a reaction time 12 h. ^b without NH₃ nor any other H₂ acceptor.

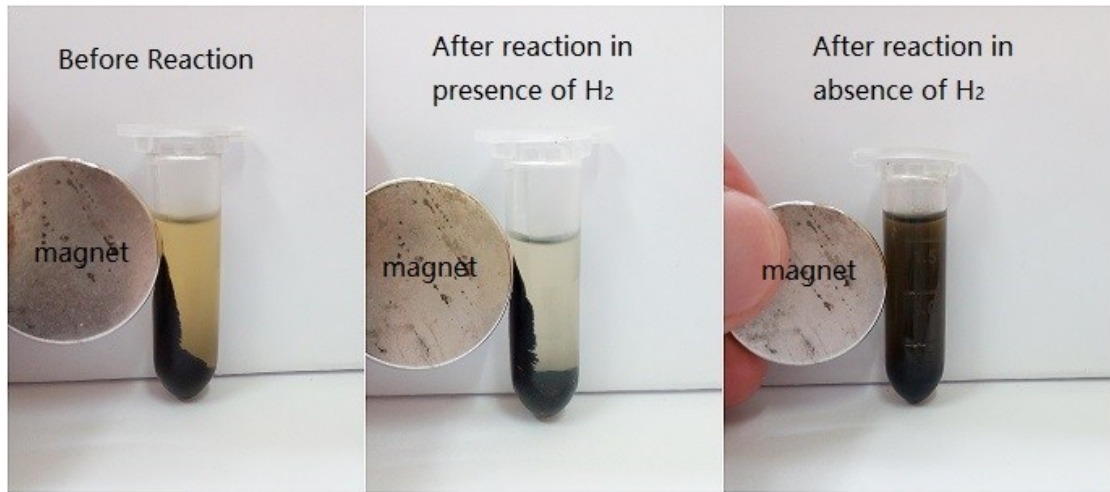


Fig. S2 The magnetic properties of the catalyst before and after the reaction

Before the reaction, Raney nickel catalyst can be attracted by the magnet, due to the magnetism of metallic nickel (left image). After the reaction in presence of hydrogen, the catalyst can also be attracted by the magnet, indicating that the nickel phase did not change during the reaction process. However, after the reaction in absence of hydrogen, the catalyst lost magnetism and cannot be attracted, intuitively showing the change of the nickel phase.

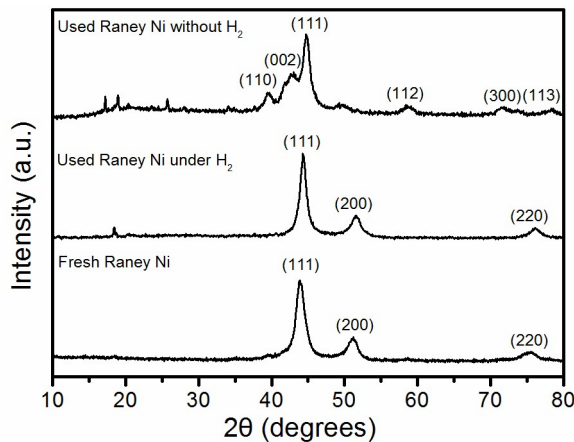


Fig. S3 X-ray diffraction patterns of fresh Raney Ni, used Raney Ni under 1.0 H₂ and Used Raney Ni without H₂

The used Raney Ni in presence of H₂ has the same diffraction peaks at $2\theta = 44.4^\circ$ (Ni 111), 51.8° (Ni 200) and 76.4° (Ni 220) with fresh Raney, indicating that Raney Ni was stable in H₂-involved reductive amination reactions. The used Raney Ni in absence of H₂ exhibited different diffraction peaks at $2\theta = 38.9^\circ$, 42.1° , 44.5° , 58.5° , 70.6° and 78.4° , which corresponding to the Ni₃N (110), (002), (111), (112), (300) and (113) crystal plane (JCPDS-ICDD Card No. 10-0280), indicating the formation of Ni₃N.

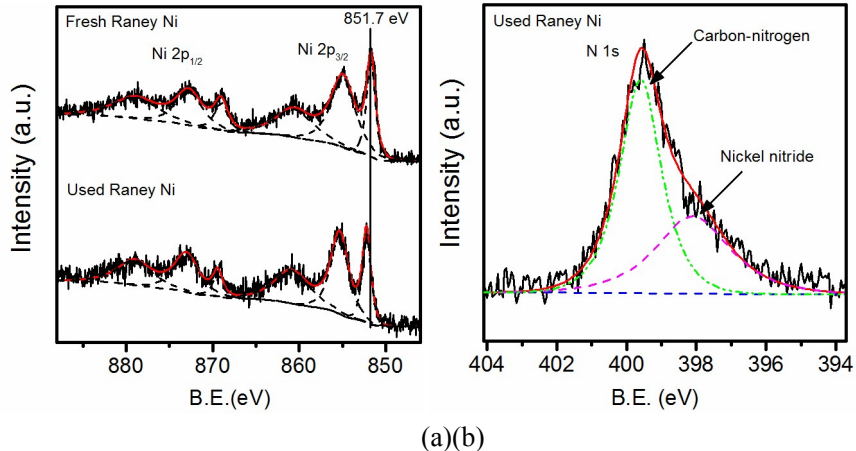


Fig. S4 High-resolution XPS spectra of Ni 2p and N 1s for used Raney Ni without H₂.

The Ni 2p_{3/2} peak at 851.7 eV and Ni 2p_{1/2} peak at 869.0 eV can be assigned to the Ni-Ni bond; the Ni 2p_{3/2} peak at 854.9 eV with a shake-up peak at 860.6 eV and Ni 2p_{1/2} peak at 872.7 eV with a shake-up peak at 878.9 eV can be assigned to the Ni-O bond, indicating that the fresh Raney Ni surface may be partially oxidized.

The used Raney Ni in absence of H₂ presented similar spectrum with the fresh Raney Ni while some differences are observed. Firstly, the peak of Ni-Ni bond shifted to a higher binding energy (852.2 eV) in the former catalyst, suggesting Ni-N bond may be formed since Ni₂N is more electron deficient than metallic nickel. This was further confirmed by the N 1s peak in which two binding energies can be distinguished. The peak at 399.6 eV corresponds to C-N bond, which can be ascribed to the adsorbed amino compounds. And the peak at 398.1 eV was generally attributed to the Ni-N bond, confirming the formation of nickel nitride.³⁵⁻³⁹

DFT calculation details

The adsorption energy of NH₃ and H₂ on metal surfaces have been studied to analyze the best catalyst for furfuryl alcohol amination. DFT calculations were carried out on Rh, Ru, Pt, Pd, Co and Ni metal surfaces. A close-packed HCP(0001) surface was used to model the flat surface of Ru, while a FCC(111) surface was used for Rh, Pt, Pd, Co and Ni. Since the HCP(0001), FCC(111) structures are close-packed, these surfaces have the lowest energy of all surfaces and therefore they are most common on nano-particles or polycrystalline surfaces. For all calculations, a 2×2 supercell model including five atomic layers are employed. A 15 Å vacuum layer between the slabs to prevent spurious interactions generated by periodic boundary conditions is used. The three bottom metal layers were fixed and the top 2 layer was allowed to relax.

All the calculations were carried out using the DMol3 program package in Materials Studio⁴⁰⁻⁴². The core treatment was set to DFT semi-core pseudopotentials (DSPP). The exchange-correlation functional of generalized gradient approximation (GGA) which can give better results for the adsorption energy⁴³ based on the PBE functional form proposed by Perdew and Burke⁴⁴ was used, where the spin-polarization was always allowed. A double numerical plus polarization (DNP)⁴⁵ basis set was employed to describe the valence orbitals of all the atoms. Brillouin-zone integrations were performed using 2×2×1 k-points grid which was generated automatically using the Monkhorst-Pack method⁴⁶. A Fermi smearing of 0.005 Ha was used to improve the calculation performance. The tolerances of energy, gradient, and displacement convergence were 1×10⁻⁵ Ha, 2×10⁻³Ha/Å, and 5×10⁻³Å respectively.

The adsorption energy of the ammonia is calculated with the following equitation:

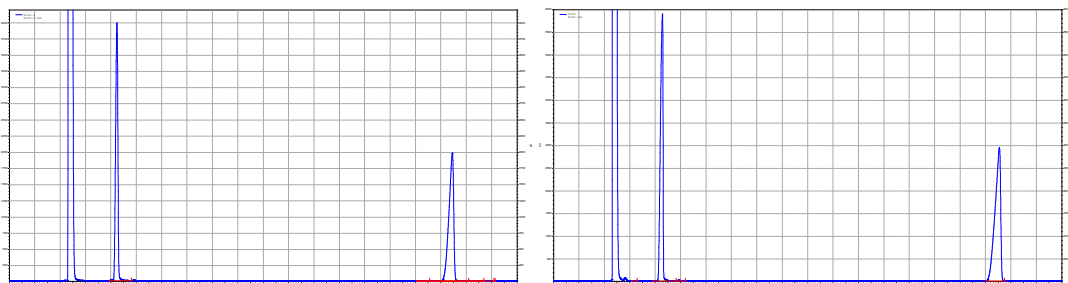
$$\Delta E = - (E_{total} - E_{metal(111)} - E_{NH_3}) \quad (1)$$

The adsorption energy of the hydrogen is calculated with the following equitation:

$$\Delta E = - (E_{total} - E_{metal(111)} - 0.5E_{H_2}) \quad (2)$$

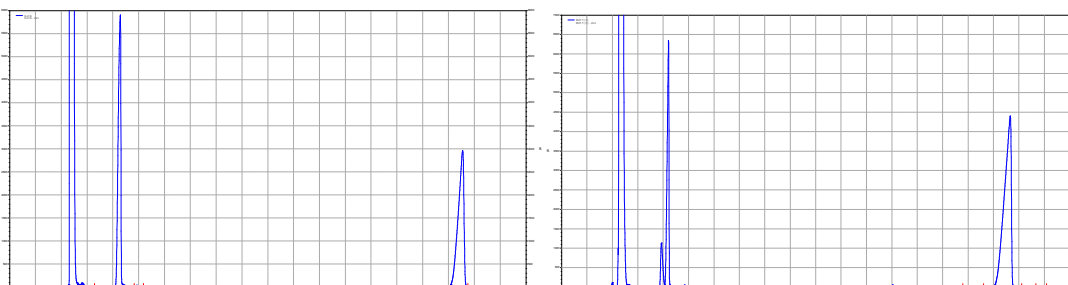
Where E_{total} is the energy of the ammonia or hydrogen on the surface, E_{metal(111)} is the energy of the metal without the hydrogen or ammonia, E_{NH₃} is the energy of ammonia in gaseous state and E_{H₂} is the energy of hydrogen in gaseous state.

Carbon balance analysis



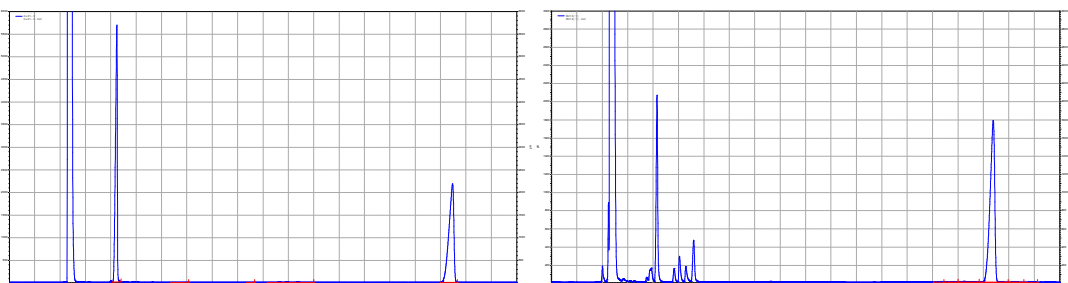
(a) Rh/C catalyzed reductive amination of FA in absence of H₂.

Reaction conditions: FA, 0.5 g; THF, 15 ml; Rh/C, 0.25 g; NH₃ pressure, 0.35 MPa; temperature, 160 °C; reaction time, 24 h; stirring speed, 1200 rpm.



(b) Raney Ni catalyzed reductive amination of FA in absence of H₂.

Reaction conditions: FA, 0.5 g; THF, 15 ml; Raney Ni, 0.25 g; NH₃ pressure, 0.35 MPa; temperature, 160 °C; reaction time, 24 h; stirring speed, 1200 rpm.



(c) Raney Ni catalyzed reductive amination of FA in 1.0 MPa H₂.

Reaction conditions: FA, 0.5 g; THF, 15 ml; Raney Ni, 0.25 g; NH₃ pressure, 0.35 MPa; H₂ pressure 1.0 MPa; temperature, 200 °C; reaction time, 12h; stirring speed, 1200 rpm.

Table S4 Summary of the above reaction results

Entry	component content (mol%)								Carbon balance
					Other by-products			unidentified compounds	
	NH ₂	OH		NH ₂					
a	-	99.5	-	-	-	-	-	-	99.5
b	20.1	76.4	-	-	-	-	-	-	96.5
c	3.9	45.1	3.2	10.2	5.4	19.1	7.9	-	94.8

f_{FA}=3.56; f_{FAM}=3.1; f_{THFAM}= 3.08; the correction factors of other compounds were approximately set as that of FA, 3.56.

The correction factors are calculated as:

$$f_i = \frac{A_s}{A_i} \cdot \frac{M_i}{M_s}$$

where A_i and M_i are the peak area and molar concentration of the component, respectively; A_s and M_s are the peak area and molar concentration of *n*-dodecane, respectively.

the molar contents of the components in the reaction bulk were then calculated as:

$$w_i = f_i \cdot \frac{A_i}{A_s} \cdot \frac{M_s}{M}$$

From Table S4, the carbon recovery is great than 94.8%, indicating our GC method for conversion and yield calculation is valid.

References

1. G. Novell-Ieruth, A. Valcárcel, J. Pérezramírez and J. M. Ricart, *J. Phys. Chem. C*, 2007, **111**, 860-868.
2. Z. P. Liu, P. Hu and M. H. Lee, *J. Chem. Phys.*, 2003, **119**, 6282-6289.
3. C. Popa, W. K. Offermans, R. A. V. Santen and A. P. J. Jansen, *Phys.Rev.B*, 2006, **74**, 137-173.
4. F. Frechard, R. A. V. Santen, A. Siokou, J. W. Niemantsverdriet and J. Hafner, *J. Chem. Phys.*, 1999, **111**, 8124-8130.
5. Á. Logadóttir and J. K. Nørskov, *J. Catal.*, 2003, **220**, 273-279.
6. C. J. Zhang, M. Lynch and P. Hu, *Surf. Sci.*, 2002, **496**, 221-230.
7. K. M. Neyman, M. Staufer, V. A. Nasluzov and N. Rösch, *J. Mol. Catal. A: Chem.*, 1997, **119**, 245-251.
8. G. Novell-Leruth, A. Valcarcel, A. Clotet, J. M. Ricart and J. Pérez-Ramírez, *J. Phys. Chem. B*, 2005, **109**, 18061.
9. W. K. Offermans, A. P. J. Jansen and R. A. van Santen, *Surf. Sci.*, 2006, **600**, 1714-1734.
10. G. Novell-Leruth, J. M. Ricart and J. Pérez-Ramírez, *J.Phys.Chem.C*, 2008, **112**, 13554-13562.
11. D. C. Ford, Y. Xu and M. Mavrikakis, *Surf. Sci.*, 2005, **587**, 159-174.
12. S. Stolbov and T. S. Rahman, *Physics*, 2005, **165**, 781-789.
13. J. Zhao, Q. Pan, M. Li, T. Yan and T. Fang, *Appl. Surf. Sci.*, 2014, **292**, 494-499.
14. J. A. Herron, S. Tonelli and M. Mavrikakis, *Surf. Sci.*, 2012, **606**, 1670-1679.
15. X. Duan, J. Ji, G. Qian, C. Fan, Y. Zhu, X. Zhou, D. Chen and W. Yuan, *J. Mol. Catal. A: Chem.*, 2012, **357**, 81-86.
16. A. C. Kizilkaya, J. W. Niemantsverdriet and C. J. Weststrate, *J. Phys. Chem. C*, 2016, **120**, 3834-3845.
17. T. Kurten, M. Biczysko, T. Rajamäki, K. Laasonen and L. Halonen, *J. Phys. Chem. B*, 2005, **109**, 8954-8960.
18. X. Duan, G. Qian, C. Fan, Y. Zhu, X. Zhou, D. Chen and W. Yuan, *Surf. Sci.*, 2012, **606**, 549-553.
19. B. Diawara, L. Joubert, D. Costa, P. Marcus and C. Adamo, *Surf. Sci.*, 2009, **603**, 3025-3034.
20. E. Sälli, V. Hänninen and L. Halonen, *J.Phys.Chem.C*, 2010, **114**, 4550-4556.
21. L. Kristinsdóttir and E. Skúlason, *Surf. Sci.*, 2012, **606**, 1400-1404.
22. S. Wilke, *Phys. Rev. B*, 1994, **50**, 2548-2560.
23. L. Xu, H. Y. Xiao and X. T. Zu, *Chem. Phys.*, 2005, **315**, 155-160.
24. G. W. Watson, R. P. K. Wells, D. J. Willock and G. J. Hutchings, *Chem. Commun.*, 2000, **8**, 705-706.
25. G. W. Watson, R. P. K. Wells, D. J. W. And and G. J. Hutchings, *J. Phys. Chem. B*, 2001, **105**, 4889-4894.
26. R. A. Olsen, G. J. Kroes and E. J. Baerends, *J. Chem. Phys.*, 1999, **111**, 11155-11163.
27. I. Hamada and Y. Morikawa, *J. Phys. Chem. C*, 2008, **112**, 10889-10898.
28. W. Dong, V. Ledentu, P. Sautet, A. Eichler and J. Hafner, *Surf. Sci.*, 1998, **411**, 123-136.
29. C. Chizallet, G. Bonnard, E. Krebs, L. Bisson, C. Thomazeau and P. Raybaud, *J. Phys. Chem. C*, 2011, **115**, 12135-12149.
30. L. Zhou, Y. Zhao, Z. Chen, G. Fu and H. Wan, *Sci.Chin.Chem.*, 2014, **58**, 156-161.
31. P. van Helden, J. A. van den Berg and C. J. Weststrate, *ACS Catal.*, 2012, **2**, 1097-1107.
32. D. J. Klinke II, S. Wilke and L. J. Broadbelt, *Surf. Sci.*, 1999, **425**, 334-342.
33. G. Kresse and J. Hafner, *Surf. Sci.*, 2000, **459**, 287-302.

34. J. F. Paul and P. Sautet, *Surf. Sci.*, 1996, **356**, L403–L409.
35. M. Shalom, D. Ressnig, X. Yang, G. Clavel, T. P. Fellinger and M. Antonietti, *J. Mater. Chem. A*, 2015, **3**, 8171-8177.
36. B. Lu, J. Li, G. Lv, Y. Qi, Y. Wang, T. Deng, X. Hou and Y. Yang, *RSC Adv.*, 2016, **6**, 93956-93962.
37. S. H. Gage, B. G. Trewyn, C. V. Ciobanu, S. Pylypenko and R. M. Richards, *Catal. Sci. Technol.*, 2016, **6**, 4059-4076.
38. S. H. Gage, D. A. Ruddy, S. Pylypenko and R. M. Richards, *Catal. Today*, 2016, DOI: 10.1016/j.cattod.2016.12.016.
39. K. J. Soo, M. A. Park, J. Y. Kim, P. S. Ha, C. D. Young, S. H. Yu, J. Kim, J. Park, J. W. Choi and L. K. Jae, *Sci. Rep.*, 2015, **5**, 10450.
40. B. Delley, *Journal of Physical Chemistry*, 1996, **100**, 6107-6110.
41. B. Delley, *J. Chem. Phys.*, 2000, **113**, 7756-7764.
42. B. Delley, *Phys. Rev. B*, 2002, **66**.
43. P. Hu, D. A. King, S. Crampin, M. H. Lee and M. C. Payne, *Chem. Phys. Lett.*, 1994, **230**, 501-506.
44. J. P. Perdew, K. Burke and M. Ernzerhof, *Phys. Rev. Lett.*, 1996, **77**, 3865-3868.
45. Y. Inada and H. Orita, *J. Comput. Chem.*, 2008, **29**, 225-232.
46. H. J. Monkhorst and J. D. Pack, *Phys. Rev. B*, 1976, **13**, 5188-5192.